

A Simple Shell Model for Quantum Dots in a Tilted Magnetic Field

W.D. Heiss* and R.G. Nazmitdinov*,**

* Centre for Nonlinear Studies and Department of Physics
University of the Witwatersrand, PO Wits 2050, Johannesburg,
South Africa

** Bogoliubov Laboratory of Theoretical Physics
Joint Institute for Nuclear Research, 141980 Dubna, Russia

A model for quantum dots is proposed, in which the motion of a few electrons in a three-dimensional harmonic oscillator potential under the influence of a homogeneous magnetic field of arbitrary direction is studied. The spectrum and the wave functions are obtained by solving the classical problem. The ground state of the Fermi-system is obtained by minimizing the total energy with regard to the confining frequencies. From this a dependence of the equilibrium shape of the quantum dot on the electron number, the magnetic field parameters and the slab thickness is found.

PACS numbers: 73.20 Dx, 73.23.Ps

I. INTRODUCTION

Recent progress in semiconductor technology now allows the fabrication of artificially structured atoms in semiconductors called quantum dots, in which electrons are trapped in a small localized region of space of a few hundred Angströms. In these nanostructures the electron wavelength is of the same length scale as the confinement so that quantum effects are important, which results in the quantization of single-electron energy levels with excitation energy of several meV (see for review¹⁻³). A prominent feature of a Fermi-system which is confined to a finite region of space is the emergence of shell effects in the single-particle spectrum as is well known in nuclear physics⁴ and more recently for large metallic clusters (⁵⁻⁸ and references therein). In the present work we address this problem to mesoscopic systems like quantum dots which contain a small number of electrons.

The electron states of few-electron quantum dots subjected to a strong magnetic field have been studied extensively in⁹⁻¹⁴. The electrodynamic response of an interacting electron system in the presence of a confining potential is expected to be dominated by the many-body effects of the electrons. Sikorski and Merkt⁹ found experimentally the surprising result that the resonance frequencies in the magneto-optical spectrum are independent of the number of electrons in the quantum dot. The systems which are experimentally realized extend much less in the z -direction than in the $x - y$ -plane. This has led to a simple description of the far-infrared resonance (FIR) frequencies¹⁵⁻¹⁷ as the energy levels of a two-dimensional harmonic oscillator potential in the presence of a magnetic field¹⁸. It was interpreted as a consequence of Kohn's theorem¹⁹ which has been generalized for a parabolic potential^{15-17,20-22}. According to this theorem, the total Hamiltonian can be divided into two parts, the center-of-mass motion (CM) and the relative motion which contains the electron-electron interaction. Since the radiation of an external electric dipole

field couples only to the CM motion and does not affect the relative motion, the dipole resonance frequencies for the interacting system should be exactly the same as those of the noninteracting system and be independent of the electron-electron interaction.

A full understanding of the experimental results needs an analysis of many-body effects. Microscopic calculations using Hartree approximation for electron numbers $N < 10^{23}$ neglected the exchange and correlation effects. The direct numerical diagonalization¹⁷ have been performed only for three- and four electron systems. The more complicated resonance structure observed in^{11,14} raised the question as to the validity of Kohn's theorem for quantum dots. In order to describe the experimental data it was assumed that, in real samples, there is a deviation of the confining potential from the parabolic form, and different corrections have been introduced^{24,25}. Also, the important role of the combined effect of the Coulomb forces and spin interaction leading to a redistribution of single-electron levels was demonstrated for the whole energy spectrum, especially for the low-lying single-electron states in the homogeneous magnetic field^{26–28}. The ground state transitions predicted in this way have been observed experimentally¹³.

It seems therefore natural to assume that the properties of the electron states close to the Fermi level are determined by an effective mean field. It is true that the external field is the dominant part of the mean field, and thus the effective confining potential should reflect the main features of it. Yet it must also contain the effect of the interplay between Coulomb forces and the external fields which are governed by the charges in the adjacent layers and gates and the magnetic field. Due to these considerations, we assume that the confining potential should also take into account the changes that affect the properties of the single-electron states owing to a variation of the homogeneous magnetic field as well as the slab thickness.

Based on the results discussed in²⁹ we conclude that the harmonic oscillator potential can serve as one of the phenomenological effective confining potentials in real samples, at least for small electron numbers. In this paper we study a simple model of a three-dimensional quantum dot in an arbitrarily oriented magnetic field for electron numbers for which the assumption of a parabolic type potential is still physically reasonable. Our procedure invokes an effective dependence of the parameters of the confining potential on the magnetic field. In this way, we accommodate the different mechanisms mentioned above and we allow the system to adjust and change its shape under variation of the applied magnetic field and the particle number. We assume that the electron system behaves like an isolated yet confined droplet (see also discussion in³⁰). One of the major result is a dependence of the single-electron states on the slab thickness. Such dependence shows in the FIR frequencies on which our analysis is focussed. We also report on transition strengths in absorption experiments and on the spatial extension of the confining potential in a quantum dot. Preliminary results have been reported in³¹.

II. THE MODEL

We consider the Hamiltonian for N noninteracting electrons moving in an effective mean field, i.e. a three-dimensional harmonic oscillator

$$H = \frac{1}{2m} \sum_{j=1}^N (\vec{p}_j - \frac{e}{c} \vec{A}_j)^2 + \frac{m}{2} \sum_{j=1}^N (\omega_x^2 x_j^2 + \omega_y^2 y_j^2 + \omega_z^2 z_j^2) \quad (1)$$

with $\vec{A} = [\vec{B} \times \vec{r}]/2$ being the vector potential associated with the homogeneous magnetic field \vec{B} . The model does not explicitly take into account spin degrees of freedom. In other words, the system is assumed to be in a fixed spin state of an arbitrary degree of polarisation. Only the orbital motion is affected by the magnetic field. Using quantum mechanical equations of motion Yip²¹ calculated resonance frequencies for this model. Our approach is similar in spirit to²¹, but we first solve the classical problem, from which all quantum mechanical results easily follow. In contrast to^{21,22} where the FIR frequencies are completely determined by the external potential, the effective mean field responds in our approach to the change of the magnetic field and particle number and thus affects the properties of single-particle excitations. We determine the frequencies ω_i , $i = x, y, z$ by minimizing the total energy for a given number of electrons N . In this way we allow the system to adjust the shape of the confining potential under the influence of the applied magnetic field and the particle number.

The classical equations of motion for the cartesian components of the momentum and position coordinates read

$$\frac{d}{dt} \begin{pmatrix} \vec{p} \\ \vec{r} \end{pmatrix} = \mathcal{M} \begin{pmatrix} \vec{p} \\ \vec{r} \end{pmatrix} \quad (2)$$

where \vec{p} and \vec{r} are combined to the six dimensional column vector denoted below as $\{\vec{p}, \vec{r}\}$. The matrix \mathcal{M} is given by

$$\mathcal{M} = \begin{pmatrix} 0 & -\Omega_z & \Omega_y & -\omega_x^2 - \Omega_y^2 - \Omega_z^2 & \Omega_x \Omega_y & \Omega_x \Omega_z \\ \Omega_z & 0 & -\Omega_x & \Omega_x \Omega_y & -\omega_y^2 - \Omega_x^2 - \Omega_z^2 & \Omega_y \Omega_z \\ -\Omega_y & \Omega_x & 0 & \Omega_x \Omega_z & \Omega_y \Omega_z & -\omega_z^2 - \Omega_x^2 - \Omega_y^2 \\ 1 & 0 & 0 & 0 & -\Omega_z & \Omega_y \\ 0 & 1 & 0 & \Omega_z & 0 & -\Omega_x \\ 0 & 0 & 1 & -\Omega_y & \Omega_x & 0 \end{pmatrix} \quad (3)$$

where the notation $\vec{\Omega} = e\vec{B}/(2mc)$ is used. Denoting the eigenvalues of \mathcal{M} by $\pm iE_k$, $k = 1, 2, 3$ we obtain from the form $\mathcal{M} = \mathcal{U}\mathcal{D}\mathcal{V}$ the classical solution

$$\{\vec{p}(t), \vec{r}(t)\} = \mathcal{U} \exp(\mathcal{D}t) \mathcal{V} \{\vec{p}(0), \vec{r}(0)\} \quad (4)$$

where $\mathcal{D} = \text{diag}(-iE_1, -iE_2, -iE_3, iE_3, iE_2, iE_1)$. While the classical orbits are of little interest in the present context, the eigenmodes E_k and the system of eigenvectors listed in the matrix \mathcal{U} are essential for the quantum mechanical treatment.

The eigenmodes which are usually referred to as the normal modes are obtained from the secular equation

$$\det |EI - \mathcal{M}| = 0 \quad (5)$$

with I denoting the six-dimensional unit matrix. The above equation turns out to be a third order polynomial in E^2 and has also been found by²¹. The column vectors of \mathcal{U} are the (complex) right hand eigenvectors of \mathcal{M} (note that \mathcal{M} is not symmetric, hence neither \mathcal{U} nor \mathcal{V} are unitary, yet $\mathcal{V} = \mathcal{U}^{-1}$). We denote the column vectors of \mathcal{U} by $u^{(k)}$, they obey the equations

$$\begin{aligned} (\mathcal{M} + iE_k I)u^{(k)} &= 0, \quad k = 1, 2, 3 \\ (\mathcal{M} - iE_{7-k} I)u^{(k)} &= 0, \quad k = 4, 5, 6 \end{aligned} \quad (6)$$

which can be solved as an inhomogeneous system by choosing for instance the sixth component of $u^{(k)}$ equal to unity and then determining the normalisation as described in Appendix A. With the proper normalisation the classical Hamilton function of Eq.(1) is cast into the quantum mechanical form

$$H = \sum_k^3 \hbar E_k (Q_k^\dagger Q_k + \frac{1}{2}). \quad (7)$$

The normal mode boson operators Q^\dagger and Q are related to the quantised version of the classical coordinates by

$$\{\vec{p}, \vec{r}\} = \mathcal{U}\{Q, Q^\dagger\}, \quad (8)$$

where we denote by $\{Q, Q^\dagger\}$ a column vector which is the transpose of the vector $(Q_1, Q_2, Q_3, Q_3^\dagger, Q_2^\dagger, Q_1^\dagger)$. The properties of the matrix \mathcal{U} guarantee the commutator $[Q_k, Q_{k'}^\dagger] = i\hbar \delta_{k,k'}$ as a consequence of $[x_i, p_j] = i\hbar \delta_{i,j}$. We note that Eq.(7) is the exact quantised equivalent of Eq.(1).

III. QUANTUM ENERGY MINIMISATION

The total energy of an N -particle system associated with the Hamiltonian Eq.(7) is given by

$$E_{\text{tot}} = \sum_{j,k} \hbar E_k (n_k + 1/2)_j. \quad (9)$$

The occupation numbers n_k are the eigenvalues of $Q_k^\dagger Q_k$ and take the values $0, 1, 2, \dots$. The ground state is determined by filling the single-particle levels $\sum_k \hbar E_k (n_k + 1/2)$ from the bottom. We take care of the electron spin only in obeying the Pauli principle which allows two particles in one level. It is clear that different sets of normal modes yield different sets of occupation numbers. The normal modes depend on the three components of the magnetic field and on the harmonic oscillator frequencies. From our assumption that the system adjusts itself under the influence of the magnetic field by minimising E_{tot} , a variation of the magnetic field strength leads to a corresponding change of the confining effective potential which is given by the oscillator frequencies. In other words, for a given magnetic field, we must seek the minimum of E_{tot} under variation of the oscillator frequencies. The variation cannot be unrestricted as

the confining potential encloses a fixed number of electrons, and assuming that the electron density does not change we are led to a fixed volume constraint which translates into the subsidiary condition $\omega_x \omega_y \omega_z = \omega_0^3$ with ω_0 fixed. Denoting the Lagrange multiplier by λ we solve the variational problem

$$\delta(\langle g|H|g\rangle - \lambda \omega_x \omega_y \omega_z) = 0 \quad (10)$$

where $|g\rangle$ denotes the ground state as described above.

From Eq.(10) we obtain, after differentiation with respect to the frequencies and using Feynman's theorem³²

$$\frac{d}{d\omega_k} \langle g|H|g\rangle = \langle g|\frac{dH}{d\omega_k}|g\rangle, \quad (11)$$

the useful condition

$$\omega_x^2 \langle g|x^2|g\rangle = \omega_y^2 \langle g|y^2|g\rangle = \omega_z^2 \langle g|z^2|g\rangle \quad (12)$$

which must be obeyed at the minimum of E_{tot} .

In this paper we restrict ourselves to consideration of a thin slab which extents essentially in two dimensions. This is achieved by varying only ω_x and ω_y in the minimization procedure while keeping ω_z fixed at a value which is, say, five times larger than the other two frequencies. In this case only $\omega_x^2 \langle g|x^2|g\rangle = \omega_y^2 \langle g|y^2|g\rangle$ can be fulfilled. Choosing different (fixed) values of ω_z allows to study the dependence of the results on the slab thickness.

It is known from the two-dimensional isotropic harmonic oscillator that shell closing occurs for Fermions at the numbers 2, 6, 12, 20, 30, ... At these numbers strong shell effects manifest themselves as the most stable quantum configurations. As a consequence, for $\omega_z \gg \omega_x$ and $B = 0$ we must expect the minimum of E_{tot} at the symmetric condition $\omega_x = \omega_y$ for such electron numbers. In the mean field approach, the breaking of spherical symmetry of the potential gives rise to a deformed shape (Jahn-Teller effect³³). For example, rotational spectra of nuclei and fine structure in the mass spectra of metallic clusters are explained as a consequence of deformed equilibrium potentials of these systems (see^{4,8}). Therefore, for numbers between the shell numbers a deformed configuration ($\omega_x \neq \omega_y$) can be expected; we note that there are always two symmetric solutions: $\omega_x > \omega_y$ and $\omega_x < \omega_y$. The condition $\omega_z \gg \omega_x$ ensures that we have a genuine two-dimensional problem in that no particle occupies a quantum mode in the z -direction ($n_z = 0$). However, if the slab is made thicker (ω_z smaller), the occupation of the first mode ($n_z = 1$) will occur at the top end of the occupied levels, which could mean that we find then the symmetric minimum at 8, 14, 22, ..., since two particles are occupying the z -mode that has become available. The distinction between a slab, that is sufficiently thin so as to prevent occupation of the first mode in the z -direction, and the slab which can accommodate the first mode is seen physically in the degeneracy of the two lowest normal modes at $B = 0$. An estimate for ω_z^0 (see Appendix B) which is the frequency that just forbids occupation of a z -mode is given by $\omega_z^0 \geq \omega_{\perp}(\sqrt{4N+1} - 3)/2$ with ω_{\perp} being the average of ω_x and ω_y .

IV. DISCUSSION OF RESULTS

The level spacing $\hbar\omega_0$ of the oscillator potential is determined by equating the Fermi energy ϵ_F of a free electron gas with the potential energy $V(r) = \frac{1}{2}m^*\omega_0^2 \langle r^2 \rangle$. Assuming that the radius of a quantum dot grows with $N^{1/3}$ we have $\langle r^2 \rangle = 3/5 R_0^2 N^{2/3}$. Consequently, we have chosen $\hbar\omega_0 = 1.35 N^{-1/3} \epsilon_F$ where the Fermi energy is obtained from the mean radius R_0 and effective mass of typical quantum dots; for GaAs, $R_0 = 320 \text{ \AA}$ and $m^* = 0.067 m_e$ yield $\epsilon_F = 2 \text{ meV}$. Throughout the paper we use meV as energy units, \AA for length and Tesla for the magnetic field strengths.

A. The spectrum

The three normal modes which can be discerned experimentally as excitation energies in FIR-spectroscopy¹⁴ behave in a distinctly characteristic way when the magnetic field is switched on. We recall that the values for ω_x and ω_y are fixed by minimizing E_{tot} . In Fig. 1 we display typical patterns for two different electron numbers. In both cases, ω_z is chosen so large that n_3 remains zero. Note that, when the magnetic field is switched on, the occupation numbers n_1, n_2, n_3 refer to the normal modes and can no longer necessarily be associated with an x -, y - or z -direction.

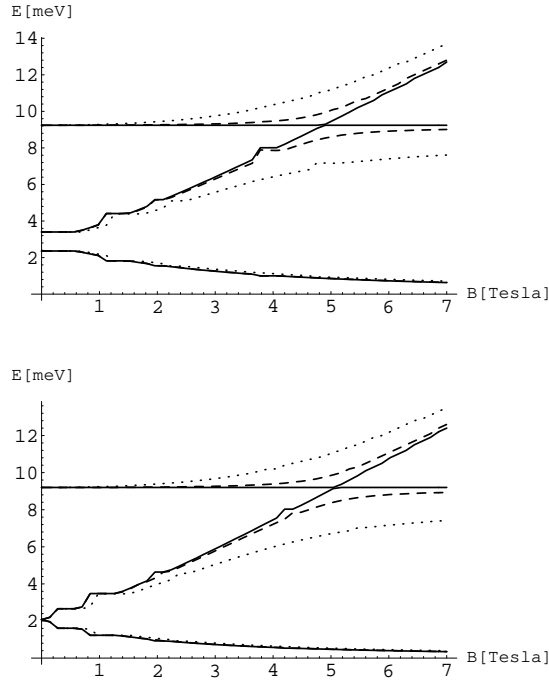


FIG. 1. Normal mode frequencies as a function of magnetic field strength for $N = 16$ (top) and $N = 30$ (bottom). Solid, dashed and dotted lines illustrate results for $\theta = 0^\circ, 10^\circ$ and 30° , respectively. Values for $\hbar\omega_z$ are 9.2 in all cases.

The degeneracy for $N = 30$ is clearly seen at $B = 0$ whereas three distinct modes, corresponding to a deformed shape, are seen at $B = 0$ for $N = 16$. The behaviour is shown for values of $\theta = 0^\circ, 10^\circ$ and 30° . For $\theta = 0$ the third mode (the highest at $B = 0$) does not interact with the applied field, therefore there is a level crossing at about $B = 5$. This becomes a level repulsion for $\theta \neq 0$ as now all modes are affected by the magnetic field. As a consequence, the

θ -dependence is strongly pronounced for the two upper modes, while such dependence is insignificant for the lowest mode. Here we find quite naturally an interpretation of avoided level crossing observed in the experiments¹⁴ associated with shape variations in a tilted magnetic field. We have also investigated the ϕ -dependence of the normal modes, which is expected to become significant only for large values of θ ; the differences are small, they can not be seen in Fig. 1. Below we return to a particular situation where the ϕ -dependence is important.

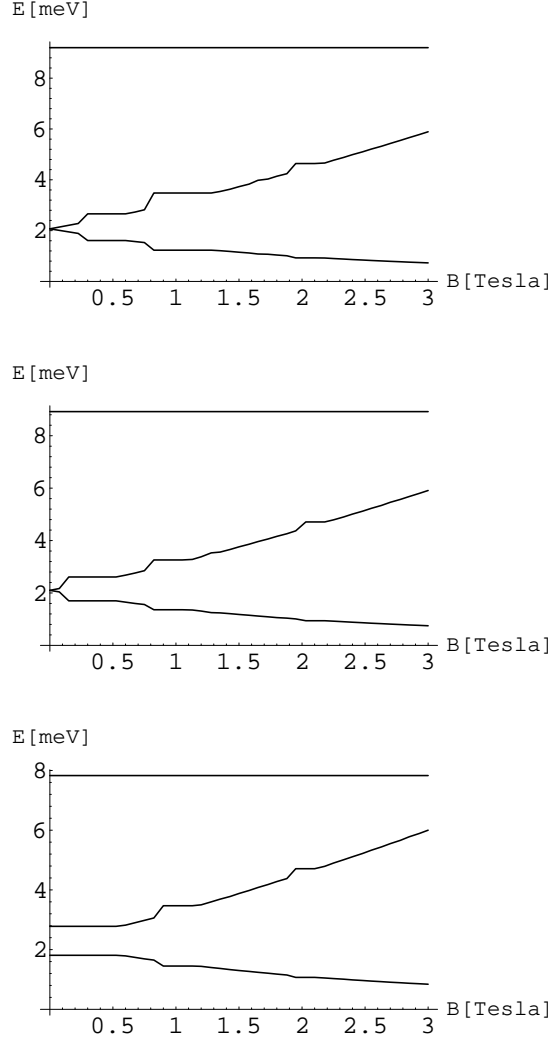


FIG. 2. Normal mode frequencies for $N = 30$ and $\theta = 0$. The slab thickness increases from the top to the bottom.

There are windows of magnetic field strength for which the normal modes are virtually constant. They are discernible especially at smaller values of the magnetic field strength and are a reflection of shape changes. For $N = 30$ the system is rotationally symmetric at $B = 0$. At $B > 0.2$ it changes into a deformed shape ($\omega_x \neq \omega_y$) which is associated with the larger derivatives of the two lower normal modes. The symmetric shape ($\omega_x = \omega_y$) is now being restored in a continuous fashion when B is further increased, the two normal modes are virtually constant during this smooth transition. The constancy of the normal modes holds strictly only for $\theta = 0$ and can be shown analytically; this is

deferred to Appendix C. At $B = 0.7$, where the system has eventually re-gained its symmetric shape, a second shape transition occurs for $B > 0.7$, which is reflected by the second sharp decrease/increase of the first/second normal mode. This pattern continues, yet it is less and less pronounced with increasing field strength. It remains to be seen whether these shape changes can be dissolved experimentally; finite temperature could disturb this pattern.

Making the slab thicker, that is choosing ω_z smaller so as to allow occupation of the next level of the third mode ($n_3 = 1$), invokes distinct changes which could possibly be dissolved experimentally. In Fig. 2 we display the effect of varying the slab thickness for $N = 30$. For clarity we focus on smaller magnetic field strength and we display only results for $\theta = 0$. The top figure is to facilitate comparison; the results are a repeat of Fig.(1b). In the middle figure the slab thickness has been decreased in such a way that the third mode becomes occupied when the field is switched on while it is unoccupied for zero field strength. As a consequence, the shape transition occurs for smaller field strength, it is here directly associated with the switch from $n_3 = 0$ to $n_3 = 1$ which is induced by the magnetic field in this particular case. The bottom figure refers to the case where $n_3 = 1$ throughout. The major effect is the lifting of degeneracy for $\vec{B} = 0$. Since there are effectively only 28 particles occupying the two lower modes, the confining potential is deformed.

With increasing field strength the potential changes into a symmetric shape which is attained at about $|\vec{B}| = 0.55$ where it again undergoes a transition to a deformed shape in line with the discussion above. In this context we note that an increase of ω_z beyond the values used in the results presented, which means an even thinner slab, pushes the upper level further away. A truly two-dimensional setting should therefore yield only two observable levels.

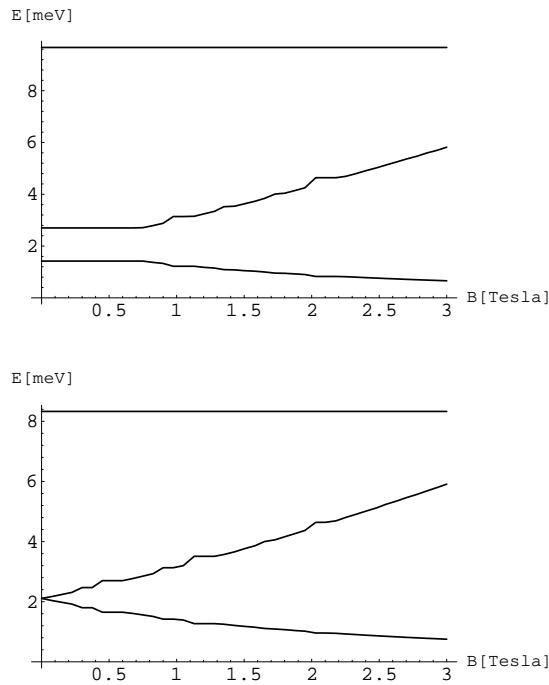


FIG. 3. Normal mode frequencies for $N = 32$ and $\theta = 0$. The slab thickness increases from the top to the bottom.

The effective occupation in the two lower modes can also be demonstrated by using $N = 22$ or $N = 32$. For $n_3 = 1$ this yields the effective numbers 20 or 30 in the planary motion with the expectation that the energy minimum is adopted for a symmetric shape. This is nicely confirmed and demonstrated in Fig. 3 where results for $N = 32$ are presented. The top and bottom figures illustrate the cases where $n_3 = 0$ and $n_3 = 1$, respectively. The interpretation is selfexplanatory after the previous discussions.

In all the examples we see quantum mechanics nicely at work. Despite the simplicity of the model, these effects should be seen in an experiment.

B. Dipole transitions

The actual observation of the three modes is achieved by electromagnetic transitions, for instance in absorption experiments. Within the single-particle model considered here transition matrix elements between the ground state and single-particle excitations are available for any single-particle operator. The electric dipole transition is expected to feature prominently. We note that this transition rules out a spin flip, which is in line with our assumption about fixed spin states. We interpret the three observed frequencies¹⁴ as the three normal modes. If no photon polarisation is measured in the initial and final states, the dipole transition strength is given by

$$S = \sum_{f, m_f, m_\gamma} |\langle f | E1 | g \rangle|^2 = \sum_{f, m_f} (|\langle f | x | g \rangle|^2 + |\langle f | y | g \rangle|^2 + |\langle f | z | g \rangle|^2), \quad (13)$$

since the electric dipole operator is proportional to \vec{r} . Using Eq.(8) the matrix elements are given by a sum over the appropriate entries of the matrix \mathcal{U} . The selection rules allow only transitions with $n_k \rightarrow n_k \pm 1$ by which all accessible final states are determined. Note that the configuration $\{n_k\}$ is different for different magnetic field strength. We list some results in Table 1. They refer to $\theta = 0$ and $n_3 = 0$ for the ground state. These figures do change as a function of θ , electron number and slab thickness. The results demonstrate that there is a redistribution of dipole strength due to variation of these parameters and therefore of the shape of the system. This aspect could be the subject of further experimental analysis.

	S	E_1	S	E_2	S	E_3
$B = 0.1$	1.0	2.0	1.0	2.1	0.7	9.2
$B = 1$	0.7	1.2	1.2	3.5	0.7	9.2
$B = 7$	0.07	0.3	0.7	9.2	1.1	12.4

Table 1. Dipole strengths S for various values of the magnetic field. The associated frequencies are indicated next to the strengths. The numbers are normalised to the lowest frequency transitions at zero field.

C. Mean square values

The calculation of matrix elements of x^2 and y^2 which are characterized by the shape of the effective confining potential follows similar lines as for the dipole matrix elements. In Table 2 we give a few values for $N = 30$ and $\theta = 0$. Note the strong deformation at $B = 0.8$. For larger field strengths the mean values decrease, since the effective frequencies of the confining potential are augmented by the Larmor frequency; this effect also enhances a symmetric shape to an increasing extent for increasing field strength. We stress that these values all obey the condition Eq.(12). For $\theta > 0$ the pattern remains essentially the same except for the fact, that the shape is not symmetric for large field strength but deformed; the degree of deformation depends on θ . This is again understood from the Larmor frequencies which are now different for the different directions. This argument is nicely confirmed when using $\theta > 0$ and $\phi = 45^\circ$; now the symmetry is guaranteed by the choice $B_x = B_y$, and, in fact, the system settles down to a symmetric configuration for large field strength. For $B = 7, \theta = 30^\circ, \phi = 0$ the mean values are 1015 and 1069, respectively, while for $\phi = 45^\circ$ they are both equal to 1044. Note that such pattern for large field strength is independent of the particle number. For instance, irrespective of the strongly deformed shape for $N = 16$ at $B = 0$, we find at $B = 7$ also a symmetric shape for $\phi = 45^\circ$ but a slight deformation for $\theta = 30^\circ$ and $\phi = 0$. Again we stress that the figures depend on the slab thickness in the spirit of the previous paragraph.

	$\sqrt{\langle g x^2 g\rangle}$	$\sqrt{\langle g y^2 g\rangle}$
$B = 0$	1167	1167
$B = 0.8$	770	1773
$B = 7$	981	981

Table 2. Mean square values of the extension in the $x - y$ -plane of the quantum dot under variation of the magnetic field strength.

V. SUMMARY

In view of the good qualitative agreement with experimental data¹⁴ we think that the model gives a fair account about the essential features of quantum dots on semiconductor interfaces. The simplicity of the soluble model allows consideration of an arbitrarily oriented magnetic field. The minimal energy requirement invokes a re-arrangement of the quantum configuration which is manifested as shell effects and hence shape changes of the quantum dot. By this mechanism we find an effective N -dependence of the FIR frequencies in quantum dots (see Fig.1). An interesting aspect of the model is the constancy of the FIR frequencies (the normal modes) under variation of the magnetic field as long as the potential is deformed. As is discussed in Section 4 the system responds to the increasing magnetic field strength by changing the confining potential towards a spherical shape rather than by changing its energy. This is shown analytically in Appendix C for $\theta = 0$ where it strictly holds. It is interesting to note that for $\theta \neq 0$ the statement still holds to high accuracy. As long as the shape of the effective confining potential is similar for different electron numbers, the splitting of the FIR frequencies due to the magnetic field should be equally alike. When the

tilting angle θ is switched on, all three modes are globally affected by the magnetic field leading to an avoided level crossing or anticrossing¹⁴. A thorough experimental analysis of a variation of slab thickness, tilted angle and strength of the magnetic field, which leads to the manifestation of quantum effects such as shape variations for fixed and different numbers of electrons, could assess the reality and limitations of the model.

The authors acknowledge financial support from the Foundation for Research Development of South Africa which was provided under the auspices of the Russian/South African Agreement on Science and Technology. R.G.N. is thankful for the warm hospitality which he experienced from the whole Department of Physics during his visit.

Note added in proof:

After submission of the present paper a report about recent experiments, which confirm essential aspects of this investigation, has appeared in Physical Review Letters, Vol. 77, 3613 (1996) by S. Tarucha, D.G. Austing, T.Honda, R.J. van der Hage and L.P. Kouwenhoven.

APPENDIX A: NORMALISATION OF THE EIGENVECTORS

The Hamilton function of Eq.(1) can be written in matrix form

$$H = \{\vec{p}, \vec{r}\}^T \mathcal{H} \{\vec{p}, \vec{r}\} \quad (\text{A.1})$$

where

$$\mathcal{H} = \begin{pmatrix} 1 & 0 & 0 & 0 & -\Omega_z & \Omega_y \\ 0 & 1 & 0 & \Omega_z & 0 & -\Omega_x \\ 0 & 0 & 1 & -\Omega_y & \Omega_x & 0 \\ 0 & \Omega_z & -\Omega_y & \omega_x^2 + \Omega_y^2 + \Omega_z^2 & -\Omega_x \Omega_y & -\Omega_x \Omega_z \\ -\Omega_z & 0 & \Omega_x & -\Omega_x \Omega_y & \omega_y^2 + \Omega_z^2 + \Omega_x^2 & -\Omega_y \Omega_z \\ \Omega_y & -\Omega_x & 0 & -\Omega_x \Omega_z & -\Omega_y \Omega_z & \omega_z^2 + \Omega_x^2 + \Omega_y^2 \end{pmatrix} \quad (\text{A.2})$$

We aim at the quantum mechanical form

$$H = \{Q, Q^\dagger\}^T \mathcal{H}_{qm} \{Q, Q^\dagger\} \quad (\text{A.3})$$

where

$$\mathcal{H}_{qm} = \begin{pmatrix} 0 & 0 & 0 & 0 & 0 & E_1 \\ 0 & 0 & 0 & 0 & E_2 & 0 \\ 0 & 0 & 0 & E_3 & 0 & 0 \\ 0 & 0 & E_3 & 0 & 0 & 0 \\ 0 & E_2 & 0 & 0 & 0 & 0 \\ E_1 & 0 & 0 & 0 & 0 & 0 \end{pmatrix}. \quad (\text{A.4})$$

Exploiting the fact that

$$\mathcal{M} = \begin{pmatrix} 0 & -I \\ I & 0 \end{pmatrix} \mathcal{H} \quad (\text{A.5})$$

where I is a 3 by 3 unit matrix, it follows that, up to normalisation factors, the matrix $\mathcal{V} = \mathcal{U}^{-1}$ can be written as

$$\mathcal{V} = \begin{pmatrix} 0 & 0 & 0 & 0 & 0 & -i \\ 0 & 0 & 0 & 0 & -i & 0 \\ 0 & 0 & 0 & -i & 0 & 0 \\ 0 & 0 & i & 0 & 0 & 0 \\ 0 & i & 0 & 0 & 0 & 0 \\ i & 0 & 0 & 0 & 0 & 0 \end{pmatrix} \mathcal{U}^T \begin{pmatrix} 0 & -I \\ I & 0 \end{pmatrix}. \quad (\text{A.6})$$

This implies that $\mathcal{U}^T \mathcal{H} \mathcal{U}$ is in fact skew-diagonal as in Eq.(A.4), and therefore \mathcal{U} can be normalised such that $\mathcal{U}^T \mathcal{H} \mathcal{U} = \mathcal{H}_{qm}$. Using Eq.(8), Eq.(A.3) follows.

APPENDIX B: ESTIMATE OF ω_z^0

Consider the energy of the three-dimensional oscillator

$$E = \hbar\omega_z(n_z + 1/2) + \hbar\omega_\perp(n_\perp + 1) = E_z + E_\perp \quad (\text{B.1})$$

where $\omega_x = \omega_y = \omega_\perp \neq \omega_z$. The condition $\omega_z \gg \omega_\perp$ ensures that we have a genuine two dimensional problem in that no particle occupies a quantum mode in the z -direction ($n_x \neq 0, n_y \neq 0, n_z = 0$), i.e. the first level with ($n_x = 0, n_y = 0, n_z = 1$) lies higher than the ones which are filled for given particle number. From the condition $E^0(n_x = n_y = 0, n_z = 1) \geq E(n_x + n_y = n_\perp \neq 0, n_z = 0)$ it follows

$$\omega_z^0 \geq n_\perp \omega_\perp \quad (\text{B.2})$$

For a two-dimensional system the number of particles (two particles per level) is $A = (N + 1)(N + 2)$ where $N = n_x + n_y = n_\perp$ is the shell number of the last filled shell. Therefore, from the equations above it follows

$$A = (n_\perp + 1)(n_\perp + 2) \quad \text{i.e.} \quad n_\perp = \frac{\sqrt{4A + 1} - 3}{2} \quad (\text{B.3})$$

Substituting Eq.(B.3) into Eq.(B.2), we obtain

$$\omega_z^0 \geq \frac{\omega_\perp}{2}(\sqrt{4A + 1} - 3) \quad (\text{B.4})$$

APPENDIX C: CONSTANCY OF THE NORMAL MODES

For $\theta = 0$ the normal modes are

$$\begin{aligned} E_1^2 &= \frac{1}{2}(\omega_x^2 + \omega_y^2 + 4\Omega_z^2 + \sqrt{(\omega_x^2 - \omega_y^2)^2 + 8\Omega_z^2(\omega_x^2 + \omega_y^2) + 16\Omega_z^4}) \\ E_2^2 &= \frac{1}{2}(\omega_x^2 + \omega_y^2 + 4\Omega_z^2 - \sqrt{(\omega_x^2 - \omega_y^2)^2 + 8\Omega_z^2(\omega_x^2 + \omega_y^2) + 16\Omega_z^4}) \\ E_3 &= \omega_z. \end{aligned} \quad (\text{C.1})$$

The last equation shows that the largest mode E_3 is independent of the magnetic field strength, since ω_z is kept fixed. From the first two equations we obtain a relation between two sets of frequencies ω_{1x}, ω_{1y} and ω_{2x}, ω_{2y} which yield the same normal modes for different field strength. With the notation $\Delta^2 = \Omega_{2z}^2 - \Omega_{1z}^2 > 0$, where Ω_{1z} and Ω_{2z} refer to the different field strengths B_1 and B_2 , we obtain from the requirements $E_{1,2}(B_1) = E_{1,2}(B_2)$

$$\begin{aligned}\omega_{2x}^2 &= \frac{1}{2}(\omega_{1x}^2 + \omega_{1y}^2 - 4\Delta^2 + \sqrt{(\omega_{1x}^2 - \omega_{1y}^2)^2 - 8\Delta^2(\omega_{1x}^2 + \omega_{1y}^2) + 16\Delta^4}) \\ \omega_{2y}^2 &= \frac{1}{2}(\omega_{1x}^2 + \omega_{1y}^2 - 4\Delta^2 - \sqrt{(\omega_{1x}^2 - \omega_{1y}^2)^2 - 8\Delta^2(\omega_{1x}^2 + \omega_{1y}^2) + 16\Delta^4})\end{aligned}\tag{C.2}$$

To ensure that ω_{2x} and ω_{2y} are real, Δ must obey the condition

$$\sqrt{\Delta} \leq \frac{|\omega_{1x} - \omega_{1y}|}{2}.\tag{C.3}$$

This means that the normal modes *must* change with the magnetic field strength for a spherical shape ($\omega_{1x} = \omega_{1y}$) as is established by the results. In turn, it is possible that E_1 and E_2 do not change under variation of B as long as $\omega_{1x} \neq \omega_{1y}$. Further, if the magnetic field strength has increased up to the value where condition (C.3) becomes an equality, then the spherical shape ($\omega_{2x} = \omega_{2y}$) is attained. Recall that throughout this transition from deformed to spherical shape the normal modes (Eq.(C.1)) have not changed.

It remains to show that this solution is in fact the minimal energy solution. For $\theta = 0$ the explicit expressions for $\langle g|x^2|g\rangle$ and $\langle g|y^2|g\rangle$ read

$$\begin{aligned}\langle g|x^2|g\rangle &= \frac{1}{2m} \left[\frac{\Sigma_1}{E_1} + \frac{\Sigma_2}{E_2} + \frac{\omega_x^2 - \omega_y^2 + 4\Omega_z^2}{E_1^2 - E_2^2} \left(\frac{\Sigma_1}{E_1} - \frac{\Sigma_2}{E_2} \right) \right] \\ \langle g|y^2|g\rangle &= \frac{1}{2m} \left[\frac{\Sigma_1}{E_1} + \frac{\Sigma_2}{E_2} + \frac{\omega_y^2 - \omega_x^2 + 4\Omega_z^2}{E_1^2 - E_2^2} \left(\frac{\Sigma_1}{E_1} - \frac{\Sigma_2}{E_2} \right) \right]\end{aligned}\tag{C.4}$$

where $\Sigma_k = \sum_j (n_k + \frac{1}{2})_j$ denotes the sum over all occupied single-particle levels. Suppose the condition Eq.(12) is fulfilled for the confining frequencies ω_{1x} and ω_{1y} for the value of the magnetic field $B_1(\Omega_{1z})$. Substituting Eqs.(C.4) into Eq.(12) and taking into account that $\omega_{1x} \neq \omega_{1y}$, we obtain

$$\left[\frac{\Sigma_1}{E_1} + \frac{\Sigma_2}{E_2} + \frac{\omega_{1x}^2 + \omega_{1y}^2 + 4\Omega_{1z}^2}{E_1^2 - E_2^2} \left(\frac{\Sigma_1}{E_1} - \frac{\Sigma_2}{E_2} \right) \right] = 0.\tag{C.5}$$

From Eqs.(C.2) it follows

$$\omega_{2x}^2 + \omega_{2y}^2 = \omega_{1x}^2 + \omega_{1y}^2 - 4(\Omega_{2z}^2 - \Omega_{1z}^2).\tag{C.6}$$

Using the result of Eqs.(C.4),(C.5) and (C.6), and the fact that Σ_1 and Σ_2 remain the same, we obtain

$$\omega_{2x}^2 \langle g2|x^2|g2\rangle - \omega_{2y}^2 \langle g2|y^2|g2\rangle =$$

$$\begin{aligned}
& (\omega_{2x}^2 - \omega_{2y}^2) \left[\frac{\Sigma_1}{E_1} + \frac{\Sigma_2}{E_2} + \frac{\omega_{2x}^2 + \omega_{2y}^2 + 4\Omega_{2z}^2}{E_1^2 - E_2^2} \left(\frac{\Sigma_1}{E_1} - \frac{\Sigma_2}{E_2} \right) \right] = \\
& (\omega_{2x}^2 - \omega_{2y}^2) \left[\frac{\Sigma_1}{E_1} + \frac{\Sigma_2}{E_2} + \frac{\omega_{1x}^2 + \omega_{1y}^2 + 4\Omega_{1z}^2}{E_1^2 - E_2^2} \left(\frac{\Sigma_1}{E_1} - \frac{\Sigma_2}{E_2} \right) \right] \equiv 0
\end{aligned} \tag{C.7}$$

where $|g2\rangle$ denotes the ground state referring to the frequencies ω_{2x}, ω_{2y} and the magnetic field B_2 . This means that Eq.(12) is fulfilled.

-
- ¹ T.Chakraborty, Comments Condens. Matter Phys. **16** 35 (1992).
² M.A. Kastner, Rev.Mod.Phys. **64**, 849 (1992).
³ N.F. Johnson, J.Phys.: Condens.Matter **7** 965 (1995).
⁴ A. Bohr and B. R. Mottelson, *Nuclear Structure* (Benjamin, New York, 1975), Vol.2.
⁵ H. Nishioka, K. Hansen, and B. R. Mottelson, Phys. Rev. **B42**, 9377 (1990).
⁶ W. A. de Heer, Rev. Mod. Phys. **65**, 611 (1993); M. Brack, *ibid* **65**, 677 (1993).
⁷ W.D. Heiss and R.G. Nazmitdinov, Phys. Rev. Lett. **73**, 1235 (1994); W.D. Heiss, R.G. Nazmitdinov and S. Radu, Phys. Rev. **B51**, 1874 (1995); W.D. Heiss, R.G. Nazmitdinov and S. Radu, Phys. Rev. **C52**, 3032 (1995).
⁸ Comments At.Mol.Phys. **31** Nos. 3-6 (1995).
⁹ Ch.Sikorski and U.Merkt, Phys.Rev.Let. **62**, 2164 (1989).
¹⁰ W.Hansen, T.P. Smith III, K.Y. Lee, J.A. Brum, C.M. Knoedler, J.M. Hong and D.P. Kern, Phys.Rev.Lett. **62**, 2168 (1989).
¹¹ T. Demel, T. Heitmann, P. Grambow and K. Ploog, Phys.Rev.Lett. **64**, 788 (1990).
¹² P.L. McEuen, E.B. Foxman, U. Meirav, M.A. Kastner, Yigal Meir, Ned S. Wingreen and S.J.Wind, Phys.Rev.Lett. **66**, 1926 (1991).
¹³ R.C. Ashoori, H.L. Stormer, J.S. Weiner, L.N. Pfeiffer, K.W.Baldwin and K.W. West, Phys.Rev.Lett. **71**, 613 (1993).
¹⁴ B.Meurer, D.Heitmann and K.Ploog, Phys.Rev. **B48**, 11488 (1993).
¹⁵ L.Brey, N.F. Johnson and B.I. Halperin, Phys.Rev. **B40**, 10647 (1989).
¹⁶ F.M. Peeters, Phys.Rev. **B42**, 1486 (1990).
¹⁷ P.A. Maksym and T. Chakraborty, Phys.Rev.Lett. **65**, 108 (1990).
¹⁸ V.Fock, Z.Phys. **47** 446 (1928); C.G. Darwin, Proc.Cambridge Philos. Soc. **27**, 86 (1930).
¹⁹ W. Kohn, Phys. Rev. **123**, 1242 (1961).
²⁰ P.Bakshi, D.A. Broido and K. Kempa, Phys.Rev. **B42**, 7416 (1990).
²¹ S.K. Yip, Phys.Rev.**B43**, 1707 (1991).
²² Q.P. Lie, K.Karrai, S.K. Yip, S.Das Sarma and H.D. Drew, Phys.Rev. **B43**, 5151 (1991).
²³ A. Kumar, S.E. Laux and F. Stern, Phys.Rev. **B42**, 5166 (1990).
²⁴ V. Gudmundsson and R.R. Gerhardts, Phys.Rev. **B43**, 12098 (1991).
²⁵ D. Pfannkuche and R.R. Gerhardts, Phys.Rev. **B44**, 13132 (1991).
²⁶ M. Wagner, U. Merkt and A.V. Chaplik, Phys.Rev. **B45**, 1951 (1992).
²⁷ P.A. Maksym and T.Chakraborty, Phys.Rev. **B45**, 1947 (1992).
²⁸ J.H.Oh, K.J.Chang, G.Ihm and S.J.Lee, Phys.Rev. **B50**, 15397 (1994).
²⁹ D. Heitmann and J. Kotthaus, Phys.Today **46**, 56 (1993).
³⁰ M.A. Kastner, Comments Condens. Matter Phys. **16**, 349 (1996).
³¹ W.D. Heiss and R.G. Nazmitdinov, Phys.Lett. **A 222**, 309 (1996).
³² R.P. Feynman, Phys.Rev. **56**, 340 (1939).
³³ H.A. Jahn and E. Teller, Proc. Roy. Soc. **A161**, 220 (1937).